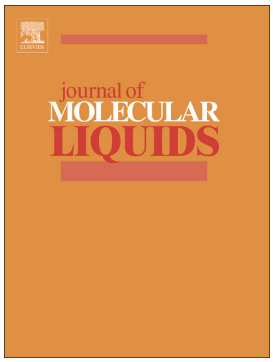

Synthesis of Ca-doped ZnO nanoparticles and its application as highly efficient electrochemical sensor for the determination of anti-viral drug, acyclovir

Davalasab Ilager, Nagaraj P. Shetti, Ramesh S. Malladi, Nitinkumar S. Shetty, Kakarla Raghava Reddy, Tejraj M. Aminabhavi

PII: S0167-7322(20)35557-4

DOI: https://doi.org/10.1016/j.molliq.2020.114552

Reference: MOLLIQ 114552

To appear in: *Journal of Molecular Liquids*

Received date: 23 August 2020

Revised date: 6 October 2020

Accepted date: 9 October 2020

Please cite this article as: D. Ilager, N.P. Shetti, R.S. Malladi, et al., Synthesis of Ca-doped ZnO nanoparticles and its application as highly efficient electrochemical sensor for the determination of anti-viral drug, acyclovir, *Journal of Molecular Liquids* (2018), https://doi.org/10.1016/j.molliq.2020.114552

Synthesis of Ca-doped ZnO nanoparticles and its application as highly efficient electrochemical sensor for the determination of anti-viral drug, acyclovir

Davalasab Ilager[a], Nagaraj P. Shetti[a]*, Ramesh S. Malladi[b], Nitinkumar S. Shetty[c], Kakarla Raghava Reddy[d]*, Tejraj M. Aminabhavi[e]

[a]*Center of Electrochemical Science and Materials, Department of Chemistry, K. L. E. Institute of Technology, Gokul, Hubballi-580027, Karnataka, India.*

[b]*Department of Chemistry, BLDEA's V.P Dr. P.G. Halakatti College of Engineering & Technology, Vijayapur-586103, Karnatak, India.*

[c]*Department of Chemistry, Manipal Institute of Technology, MAHE, Manipal-576 104, India*

[d]*School of Chemical and Biomolecular Engineering, The University of Sydney, Sydney, NSW 2006, Australia*

[e]*Pharmaceutical Engineering, SET's College of Pharmacy, Dharwad, 580-007, India*

*****Correspondence to*: reddy.chem@gmail.com (K. R. Reddy); dr.npshetti@gmail.com (N. P. Shetti)

Abstract

Recent developments to utilize nanostructured metal oxides for fabricating novel sensors with superior sensitivity have prompted advanced detection limits even at trace level. In the current study, development of calcium doped zinc oxide (Ca-ZnO) nanoparticles as a novel electroanalytical sensing tool for the detection of antiviral drug, acyclovir (ACV) was performed. Ca-ZnO nanoparticles modified sensors to enhance the electrochemical properties of ACV as compared to an unmodified glassy carbon electrode (GCE) in pH 5.0. The influence of various factors such as effect of pre-concentration time, sweep rate, and concentration on the oxidation peak current of ACV has been discussed. The experimental results showed the wide linearity range (8.0×10^{-8} M to 2.4×10^{-5} M) with lower values of detection (6.18 nM). Hence, developed novel nanosensor showed an intensification of peak current of ACV with significant sensitivity, selectivity, and reproducibility for ACV analysis and obtained results were apply for the determination of ACV in the analysis of urine and pharmaceutical dosage form.

Keywords: Ca-ZnO nanoparticles; Electrochemical sensor; Glassy carbon electrode, Acyclovir; Analytical applications

1. Introduction

Antiviral drugs are used to treat specific viral diseases, whereas a wide range of antivirals are active against a variety of viruses [1-2]. Acyclovir (ACV) is a widely used antiviral drug whose high concentration in the human body causes nausea and diarrhea along with some potentially serious side effects related to kidneys and low platelets though the drug has some beneficial effects [3-4].

Numerous analytical techniques have been reported for the analysis of ACV by spectrophotometric and spectrofluorimetric methods [5], near-infrared spectroscopy for quantitative confirmation of ACV in plasma [6], ACV and associated impurities by liquid chromatography [7] and HPLC techniques [8], radio-immuno assay [9] as well as LC/MS technique (liquid chromatography/mass spectrometry) [10]. These methods are usually complicated requiring sophisticated instruments and manual procedures, such as optimizing chromatographic conditions, pre-treatment of HPLC samples, and disposal of radioactive materials. On the other hand, electrochemical methods such as voltammetry, polarography, and amperometry offer benefits of high sensitivity, rapid response, and accurate quantification of biological as well as environmental samples [11-20].

Electrochemical sensors (chemical and biological) have an extreme effect in recent years in the fields of medical diagnosis, personal protection, agriculture and the detection of environmental toxins. In recent decades, research has focused on the creation of simple solid-state sensors whose activity is dependent on the output of a measurable signal based on the analyte's interaction with the sensor's active surface. In view of these, electrochemical techniques are well suited to evaluate the analyte in real time to report their ability to accept/donate electrons. In addition, the applicability of this approach to investigate organic and inorganic biomolecules has been noticed. In the voltammetric technique, unmodified electrodes decrease the sensitivity because of slow movement of electrons in the reaction

mechanism; metal oxide nanoparticles (NPs) can improve the performance of electrochemical sensor and binding ability for the quantification of bioactive molecules and environmental samples [21-26].

In the preparation of sensors, materials with high porosity, low electroconductivity, high stability, non-hazardous surface area, and readily available in terms of cost, magnetise the attention of electrochemists. The development of chemically modified electrodes (CME), due to their easy applicability in electrochemical cells, is very significant in recent years. Due to its rich surface formation, low background current, wide range of potential windows, and inertness, glassy carbon electrodes (GCEs) loaded with one or more modifying agents have been the subject of great interest. ZnO-based NPs have advantages of lower price, wide occurrence as well as large band gap, find a niche in many applications [27].

The ZnO is an n-type semiconductor, which has an energy band gap of 3.37 eV with an exciton binding energy of about 60 meV at room temperature. Researchers are focused on modificators for long-term stability, good electrical conductivity, large surface. Certain unique characteristics are found in the Ca–ZnO doped zinc oxide nanoparticles such as increasing of electrical conductivity by the consolidation of dopant-calcium into ZnO nanoparticles through the development of an additional transporter in a commutation route as a consequence of the doping of Ca^{2+} sites. Calcium-doped zinc oxide nanoparticles were prepared in this work through co-precipitation reaction followed by hydrothermal process. Dopant calcium plays an essential role in altering ZnO's optical and structural qualities. Ca in ZnO nanoparticles monitors molecular adsorption by aqueous solutions to ensure that the calcium acts as a donor. Hence, doped metal oxide NPs when used as biosensors, and doping can contribute greatly to achieve a suitable response and at the same time offering a lower detection limit (LOD) as well as faster electron transfer [28-30]. Looking at the enhanced electrocatalytic performance through the doping process, ACV is used in this work and the

electrochemical behavior of acyclovir at Ca-ZnO/GCE has not been reported in the literature. In view of this, we have utilized synthesized Ca doped-ZnO nanoparticles for the electrochemical sensing of antiviral drug, acyclovir. The working electrode assembly causes the oxidation of ACV by enhancing its peak current leading to an appreciable detection linearity range, lower detection limit, and limit of quantification. Importantly the sensor exhibited significant sensitivity, selectivity, and reproducibility and could be extended to detect ACV in biological urine samples and pharmaceutical formulations.

2. Experimental

2.1 Instrumentation

Cyclic and square wave voltammetric techniques were used to collect the data on the electrochemical behaviour of ACV using electrochemical analyzer (CHI Company, D630, USA). Three electrodes were connected to the electrochemical analyzer including the working electrode (Bare GCE and Ca-ZnO/GCE) on which electro-oxidation of ACV was performed, saturated Ag/AgCl as a reference electrode with 3.0 M KCl solution and an auxiliary electrode as a platinum wire was used. The pH of the solution (phosphate buffer solution) was monitored with Elico (model LI120, Mumbai, India) pH meter at 25 ± 0.1 °C.

2.2 Reagents and chemicals

Acyclovir (pure form) was received from Sigma-Aldrich as well as the analytical grade reagents from SDFCL-Chem. Ltd., Mumbai, India. ACV's stock solution was dissolved in deionized water at a concentration of (1.0 mM) and kept in a cool place until its use. The supporting buffer, 0.2 M phosphate buffer solution (PBS) with varying pH (3.0 to 11.2) was formulated according to pre-documented reports [23].

2.3. Synthesis of calcium-doped zinc oxide nanoparticles

The method of co-precipitation was used to synthesize 5 % Ca-ZnO NPs. A mixture of zinc nitrate solution ($Zn(NO_3)_2 \bullet 4H_2O$) of 0.1 M, 5% mole fraction of calcium nitrate, and 10 mg/L surfactant of sodium dodecyl sulphate (SDS) were agitated for approximately 1 h for zinc nitrate decomposition. After dissolving zinc nitrate, NaOH (0.2 M) of 100 mL solution was slowly transferred drop-wise to above reaction solution and stirred for 45 min. The particle size is restricted by the use of a capping agent (sodium dodecyl sulfate surfactant). After the addition of sodium hydroxide, the colloidal reaction mixture was allowed to proceed for 2 h, the colloidal solution was kept overnight to settle down, from which the supernatant fluid was extracted, and centrifuged to obtain the solid for about 10-15 min. Thus formed ZnO NPs were rinsed repeatedly with double distilled water and ethanol. After, NPs were dried for 4 hours (60° C). The produced particles were processed in a muffle furnace under calcination for 3 h at 500° C.

2.4. Preparation of pharmaceutical sample

The applicability of the Ca-ZnO/GCE is to investigate ACV in Acivir – 200 mg tablet containing ACV. These tablets were purchased from nearby pharmacy. Ten tablets were finely crushed using a mortar, and a portion of this powder was weighed, dissolved with the help of double-distilled water, similar to the ACV stock solution (1.0 mM). A proper volume of the prepared sample solution was analyzed under optimal conditions using the SWV technique. The amount of ACV in the drug has been determined using a calibration plot.

2.5. Preparation of urine sample

The biological samples (urine) assembled at ambient temperature (25 ± 0.1 ° C) by healthy volunteers and centrifuged for 5 min. Further solutions were diluted with pH 5.0 phosphate buffer, spiking the appropriate volume of ACV (0.1 mM) solution with urine samples was used to produce a spiked urine sample. Under optimum conditions, square wave

voltammograms were recorded. In urine samples, the contents of ACVs were estimated by the standard addition method.

2.6. Electrode preparation

Initially, GCE was prepared with pre-treatments. Reaction solution was prepared by dissolving 0.5 mg of Ca-ZnO nanoparticles by ultrasonic agitation in ethanol, then the drop casting method was employed to modify the surface of the working electrode. Ca-ZnO suspension (0.15 μL) was coated on the surface of GCE, and dried under ultrasonic wave exposure. Finally, the working electrode surface containing the coated Ca-ZnO NPs was used to obtain the voltammograms [31-32].

3. Results and discussion

3.1. Characterization of Ca-ZnO/GCE

Characterization of Ca-ZnO was done by SEM, TEM, HRTEM, XRD, and EDX techniques. Figure SI1. (A) shows TEM images of Ca-ZnO NPs that are generally found to be the spherical shape with a size of about 20-30 nm. HRTEM image of doped particles is shown in Figure SI2. Figure SI1. (B) represents SEM images of Ca-ZnO nanoparticles, indicating a huge surface area. Figure SI1. (C) shows XRD patterns of Ca-ZnO NPs with large peaks for ZnO, but for calcium species, peaks are negligibly moving towards minimal 2θ degrees. The lattice planes are harmonious with the diffraction peaks, while planes of the lattice show NPs structure, which is hexagonal wurtzite. This structure is attributed to the discrepancy between the sizes of ions of Zn and Ca, suggesting a hexagonal lattice strain owing to certain residual strain within the NPs.

The crystal's average size (d) was computed by implementing the Scherrer formula for XRD spectra. The elements, which are found in Ca-ZnO, whose atomic and mass % are shown by the EDX spectroscopy (Figure SI1. (D)). The atomic % of Ca, Zn, and

O were, respectively 3.01, 44.5, and 52.7. The Ca, Zn, and O, and the mass % of these elements were, respectively 3.0, 74.98, and 22.01. The peaks from the spectrum indicate that Ca, Zn, and O appear at 3.67, 8.59, and 0.55 keV.

The exposed surface area of the Ca-ZnO/GCE was calculated through CV technique using the Randles-Sevcik equation for the irreversible process [33]:

$$I_p = [2.69 \times 10^5 \times n^{3/2} \times A \, D_0^{1/2} \times \nu^{1/2} \times C_0^*] \quad (1)$$

For estimating the extensive surface area of the nascent and fabricated GCE, We utilized 0.1 M KCl as a supporting electrolyte in which 1.0 mM $[K_3Fe(CN)_6]$ solution is used with varying scan rates at 25 °C. From Figure 1, bare GCE surface area, ZnO/GCE and Ca-ZnO/CPE were calculated to be 0.041 cm^2, 0.073 cm^2 and 0.148 cm^2, respectively.

Here Figure 1

3.2. Electrochemical behaviour of ACV at Ca-ZnO/GCE

Voltammetric behaviour of ACV has been investigated at modified and bare GCE in pH 5.0 by CV technique. Figure 2A indicates voltammograms for 0.1 mM ACV at bare and Ca-ZnO modified electrodes. Initially, blank voltammogram of GCE and Ca-ZnO/GCE was showed the absence of a peak in cyclic voltammogram and a single oxidation peak occurred in the presence of ACV for both bare GCE (4.95 μA), ZnO/GCE (8.92 μA) and Ca-ZnO/GCE (16.82 μA) respectively. The enhancement of peak current for Ca-ZnO/GCE as compared to both bare GCE and ZnO/GCE is clearly due to the role of the dopant calcium, which might have altered the structural and optical properties of ZnO. Further, no peaks were found on the reverse scan and hence, the reaction must be irreversible in nature [34].

Here Figure 2

3.3. Variation of pre-concentration time and material loading

The time of pre-concentration effect and variation of materials loading has increased the extent of ACV adsorption at the electrode surface and thus, improved its sensitivity. Initially, pre-concentration time and amount of modifier were set between 0 to 60 seconds and 0.05 µL to 0.2 µL respectively. A enhanced peak current was found at 15 s and above 15 s, peak current decreased due to the saturation accumulation (Figure 2B) [35]. In Figure 2C, the electrode surface at 0.15 µL of Ca-ZnO showed a maximum peak current. Hence, 15 s and 0.15 µL were optimized for further investigations.

3.4. Optimization of pH

The effect of PBS was investigated in ranging between 3.0 to 11.2 pH solutions. Initially, varying the phosphate buffer solutions, an intense peak was observed in acid range 3.0 to 6.0. Here, 5.0 pH shows a maximum peak current (Fig. 3A) due to increase in the solution conductivity and ACV get oxidized with highest peak intensity [36-37]. As the solution's pH increased the potential value shifted to lower positive values (Fig. 3B) due to proton involvement in the electrode mechanism. From the plots of pH versus peak potential the equation derived was: Ep = –0.050 pH + 1.438: R^2 = 0.973. The slope value (50.0 mV/s) was close to Nernst value (59.0 mV/s), which implies that the electrode process involves an equivalent number of protons and electrons [38-39].

Here Figure 3

3.5. Variation of sweep rate

The pharmacokinetics strategies of ACV were investigated using a cyclic voltammetric technique in pH 5.0 PBS with accumulation time 15 s (Fig. 4A) and the effective scan rate was performed in the range of 0.1 – 2.0 V/s. As increasing the scan rate, peak current of the ACV was increased with a good linearity giving the fitted equation: Ip =

90.478 ν + 1.707; R^2 = 0.945 (Fig. 4B) and log I_p = 0.57 log υ + 1.88; R^2 = 0.980 (Fig. 4C), the slope value 0.57 was closer to the theoretical value of diffusion-controlled process. Hence, electro-oxidation of ACV was controlled by diffusion [40-43] and Ep (V) versus log ν (V/s) was given in Fig. 4D. For an irreversible electrode reaction of ACV, the values of α, and number electrons (n) were calculated using Eqs. (1) and (2) [44-45].

$$E_p = E^0 + \left[\frac{2.303RT}{\alpha nF}\right]\left[\frac{R\,T\,k^0}{\alpha nF}\right] + \left[\frac{2.303RT}{\alpha nF}\right]\log \nu \qquad (1)$$

$$\Delta E = E_p - E_{P/2} = \left[\frac{47.7}{\alpha n}\right] mV \qquad (2)$$

The values of α was 0.55, and the number of electrons transferred was two. In addition, using the obtained E^0 value and intercept of the plot of peak potential versus the logarithm of scan rate, k^0 was estimated to be 2.65 x 10^3 s^{-1}.

Here Figure 4

3.6. Possible electrode mechanism of ACV

Electrode mechanism of ACV on the surface Ca-ZnO modified GCE suggests the involvement of two electrons and two protons (Scheme 1). Comparing the oxidation of base ACV i.e., guanine at carbon-based electrode [46-48], we can assume that oxidation mechanism of ACV could be similar to the product (8-oxoacyclovir) as developed by the exchange of two protons and two electrons, which was identical to the initial oxidation of guanine. The suggested oxidation mechanism for ACV was given in Scheme 1.

Here Scheme 1

3.7. Detection limit of ACV

Square wave voltammetric (SWV) method was utilized to estimate the limit of detection (LOD) and quantification (LOQ) for ACV in pH 5.0 at the Ca-ZnO modified GCE (Fig. 5). When the concentration of ACV was varied in the range 0.01 μM - 24 μM, the peak current also increased. The LOD and LOQ values were determined using the calibration graph (concentration of ACV versus peak current). From the standard deviation of intercept and slope of the calibration curve, LOD and LOQ values were calculated using Eqs. 3 and 4 [49-51].

$$LOD = 3S/M \quad (3)$$

$$LOQ = 10S/M \quad (4)$$

The linearity range was found to be between 8.0 $x10^{-8}$ M and 2.4 $x10^{-5}$ M with values of lower detection and quantification was calculated to be 6.18 nM and 20.6 nM. Hence, the present approach has the benefit of a low detection limit compared to the methods previously reported (Table 1).

Here Figure 5 and Here Table 1

3.8. Effect of excipients

An excipient is a material that is formulated simultaneously along with the drug's active ingredient and hence, to promote long-term stabilization, non-sticking properties and solubility are to be tested [59-61]. The effect of some of the common excipients such as citric acid, gum acacia, oxalic acid, starch, glycine, urea, and dextrose was investigated to determine the response of ACV at Ca-ZnO/GCE surface by the SWV technique. The findings of this approach reveal that peak potential values of ACV have altered to some range, but it was not reached the ±5 % limit, indicating that the presence of used excipients may not affect ACV reactions at the senor surface (Figures 6).

Here Figure 6

4. Analytical applications

4.1. Tablet and urine sample analysis

The proposed sensor was tested using SWV to determine ACV in clinical trials such as analysis in tablet and urine samples. ACV tablet solutions were prepared as specified under section 2.3 and the results are listed in Table 2A. Good sample recoveries and low RSD % values indicate the validity of the developed sensor in biological samples for determining ACV. Further, ACV (desired amount) was spiked into human urine samples and the amount of analyte was calculated by the standard calibration plots. The present findings validate our new approach for quality assurance and therapeutic investigations. Table 2B describes the analysis results.

"Here Table 2"

4.2. Repeatability and reproducibility of Ca-ZnO/GCE

The repeatability of sensor (Ca-ZnO/GCE) was tested by evaluating 1.0 mM ACV. To achieve this, the sensor was kept for 20 days in an airtight jar. The results obtained were indicating the sensor conserved 98.2% of its actual peak current at the concentration 0.1mM of ACV, which indicates long standing reliability of Ca-ZnO/GCE. Reproductivity is related to the difference in observations provided under different conditions. Sensor reproducibility was examined in the voltammetric signals throughout the day at a constant temperature with an equivalent RSD value of 2.44%. Furthermore, sensor's reproducibility was tested at a constant temperature using an intraday study and RSD value was 1.84%, confirming the development of Ca-ZnO nanostructured materials as the foremost analytical applications to maintain good stability and reproducibility.

5. Conclusions

The present work describes the synthesis of a novel type of Ca-ZnO nanoparticles by co-precipitation method to develop a modified sensor for trace level detection of antiviral drug, ACV. The sensing surface was analyzed by SEM, EDX, TEM, and HRTEM techniques. The modified sensor was enhanced the electrochemical performance of ACV in pH 5.0 as compared to unmodified GCE. The ACV showed diffusion-controlled process with the involvement of two numbers of electrons and protons. The developed sensor provided a significant advantage for sensing ACV even at such a lower LOD (6.18 nM) value in a wide linear dynamic range (8.0 $x10^{-8}$ M to 2.4 $x10^{-5}$ M). For the determination of ACV, the SWV technique was developed and implemented for tablets and samples of human urine. Common interferents were used to analyze the interference, which suggests that the proposed approach can be suitable for adopting in clinical sample analysis.

References

[1] C. Vernassiere, A. Barbaud, P. H. Trechot, F. Weber-Muller, J. T. Schmutz, Systemic acyclovir reaction subsequent to acyclovir contact allergy: which systemic antiviral drug should then be used? Contact Dermatitis, 49 (2003)155–157.

[2] M. R. Holdiness, Contact dermatitis from topical antiviral drugs. Contact Dermatitis 44 (2001) 265–269.

[3] J. Adair, M. Gold, R. Bond. Acyclovir neurotoxicity: clinical experience and review of the literature. Southampt Med J. 87 (1994) 1227–1231.

[4] P. Singla, O. Singh, S. Chabba, R. K. Mahajan, Pluronic-SAILs (surface active ionic liquids) mixed micelles as efficient hydrophobic quercetin drug carriers, Journal of Molecular Liquids, 249 (2018) 294-303.

[5] M. M. Ayad, H. E. Abdellatef, M. M. El-Henawee, H. M. El-Sayed, Spectrophotometric and spectrofluorimetric methods for analysis of acyclovir and acebutolol hydrochloride., Spectrochim. Acta A, 66 (2007) 106-110.

[6] L. Yu, B. Xiang, Quantitative determination of acyclovir in plasma by near infrared spectroscopy, Microchem. J. 90 (2008) 63-66.

[7] A. L. Huidobro, F. J. Ruperez, C. Barbas, LC methods for acyclovir and related impurities determination, J. Pharm. Biomed. Anal. 37 (2005) 687-694.

[8] P. D. Tzanavaras, D. G. Themelis, High-throughput HPLC assay of acyclovir and its major impurity guanine using a monolithic column and a flow gradient approach. J. Pharm. Biomed. Anal. 43 (2007) 1526-1530.

[9] S. M. Tadepalli, R. P. Quinn, Scintillation proximity radioimmunoassay for the measurement of acyclovir. J. Pharm. Biomed. Anal. 15 (1996) 157-163.

[10] J. J. Sasanya, A. M. M. Abd-Alla, A. G. Parker, A. Cannavan, Analysis of the antiviral drugs acyclovir and valacyclovir-hydrochloride in tsetse flies (Glossina pallidipes) using LC–MSMS, J. Chromatogr. B. 878 (2010) 2384-2390.

[11] P. T. Kissinger, W. R. Heineman, Cyclic voltammetry, Journal of Chemical Education, 60 (1983) 702-706.

[12] H. M. Moghaddam, H. Beitollahi, S. Tajik, I. Sheikhshoaie, P. Biparva, Fabrication of novel TiO_2 nanoparticles/Mn (III) salen doped carbon paste electrode: application as electrochemical sensor for the determination of hydrazine in the presence of phenol, Environmental monitoring and assessment, 187 (2015) 1-12.

[13] J. Zheng, W. Zhang, Z. Lin, C. Wei, W. Yang, P. Dong, Y. Yan, S. Hu, Microwave synthesis of 3D rambutan-like CuO and CuO/reduced graphene oxide modified electrodes for non-enzymatic glucose detection, Journal of Materials Chemistry B, 4 (2016) 1247-1253.

[14] N. P. Shetti, S. J. Malode, D. S. Nayak, C. V. Reddy, K. R. Reddy, Novel biosensor for efficient electrochemical detection of methdilazine using carbon nanotubes-modified electrodes, Materials Research Express, 6 (2019) 116308.

[15] S. D. Bukkitgar, N. P. Shetti, R. M. Kulkarni, S. B. Halbhavi, M. Wasim, M. Mylar, P. S. Durgi, S. S. Chirmure, Electrochemical oxidation of nimesulide in aqueous acid solutions based on TiO2 nanostructure modified electrode as a sensor, Journal of Electroanalytical Chemistry, 778 (2016) 103-109.

[16] Y. Xu, X. Shi, R. Hua, R. Zhang, Y. Yao, B. Zhao, T. Liu, J. Zheng, G. Lu, Remarkably catalytic activity in reduction of 4-nitrophenol and methylene blue by Fe_3O_4@COF supported noble metal nanoparticles, Applied Catalysis B: Environmental, 260 (2020) 118142.

[17] D. Monga, D. Ilager, N. P. Shetti, S. Basu, T. M. Aminabhavi, 2D/2d heterojunction of MoS_2/g-C_3N_4 nanoflowers for enhanced visible-light-driven photocatalytic and electrochemical degradation of organic pollutants, Journal of Environmental Management 274 (2020) 111208.

[18] N. P. Shetti, S. J. Malode, D. S. Nayak, K. R. Reddy, C. V. Reddy, K. Ravindranadh Silica gel-modified electrode as an electrochemical sensor for the detection of acetaminophen, Microchemical Journal, 150 (2019) 104206.

[19] H. M. Moghaddam, H. Beitollahi, S. Tajik, M. Malakootian, H. K. Maleh, Simultaneous determination of hydroxylamine and phenol using a nanostructure-based electrochemical sensor, Environmental monitoring and assessment, 186 (2014) 7431-7441.

[20] N. P. Shetti, A. Mishra, S. Basu, R. J. Mascarenhas, R. R. Kakarla, T. M. Aminabhavi, Skin-patchable electrodes for biosensor applications: A review, ACS Biomaterials Science & Engineering, 6 (2020) 1823-1835.

[21] J. Zheng , J. Zhang , Z. Wang , L. Zhong , Y. Sun , Z. Liang , Y. Li , L. Jiang , X. Chen , L. Chi, Programmable negative differential resistance effects based on self- assembled Au@PPy core–shell nanoparticle arrays, Advanced Materials, 30 (2018) 1802731.

[22] K. Kumar, B. Avinash, M. Gorji, J. Maidoubi, Photocatalytic activity and smartness of TiO_2 nanotube arrays for room temperature acetone sensing, Journal of Molecular Liquids, 300 (2020) 112418.

[23] N. P. Shetti, S. J. Malode, D. Nager, K. R. Reddy, S. S. Shukla, T. M. Aminabhavi, A novel electrochemical sensor for detection of molinate using ZnO nanoparticles loaded carbon electrode, Electroanalysis, 31 (2019) 1040-1049.

[24] A. Aarthi, M. Umadevi, R. Parimaladevi, G. V. Sathe, Detection and degradation of leachate in groundwater using ag modified Fe_3O_4 nanoparticle as sensor, Journal of Molecular Liquids, 252 (2018) 97-102.

[25] G. Manasa, R. J. Mascarenhas, A. K. Satpati, B. M. Basavaraja, S. Kumar, An electrochemical Bisphenol F sensor based on ZnO/G nano composite and CTAB surface modified carbon paste electrode architecture, Colloids and Surfaces B: Biointerfaces, 170 (2018) 144-150.

[26] P. Bansal, G. Bhanjana, N. Prabhakar, J. Dhau, G. Chaudhary, Electrochemical sensor based on ZrO_2 NPs/Au electrode sensing layer for monitoring hydrazine and catechol in real water samples, Journal of Molecular Liquids, 248 (2017) 651-657.

[27] N. P. Shetti, S. D. Bukkitgar, R. R. Kakarla, C. V. Reddy, T. M. Aminabhavi, ZnO-based nanostructured electrodes for electrochemical sensors and biosensors in biomedical applications, Biosens. Bioelectron., 141 (2019) 111417.

[28] A. Mahmoud, M. Echabaane, K. Omri, L.E. Mir, R. B. Chaabane, Development of an impedimetric non enzymatic sensor based on ZnO and Cu doped ZnO nanoparticles for the detection of glucose, Journal of Alloys and Compounds, 786 (2019) 960-968.

[29] W. Zhang, J. Zheng, C. Tan, X. Lin, S. Hu, J. Chen, X. You, S. Li, Designed self-assembled hybrid Au@CdS core–shell nanoparticles with negative charge and their application as highly selective biosensors, Journal of Materials Chemistry B, 3 (2015) 217-224.

[30] N. P. Shetti, D. S. Nayak, S. J. Malode, R. M. Kulkarni, D. B. Kulkarni, R. A. Teggi, V. V. Joshi, Electrooxidation and determination of flufenamic acid at graphene oxide modified carbon electrode, Surfaces and Interfaces, 9 (2017) 107-113.

[31] B. Jansi Rani, G. Ravi, R. Yuvakkumar, Z. M. Hasan, S. Ravichandran, S. I. Hong, Binder free, robust and scalable CuO@GCE modified electrodes for efficient electrochemical water oxidation, Materials Chemistry and Physics, 239 (2020) 122321.

[32] D. Kumar, M. Baynosa, G. Dhakal, J. Shim, Sphere-like $Ni_3S_4/NiS_2/MoO_x$ composite modified glassy carbon electrode for the electrocatalytic determination of D-penicillamine, Journal of Molecular Liquids 2020, 301, 112447.

[33] D. Ilager, H. Seo, N. P. Shetti, S. S. Kalanur, T. M. Aminabhavi, Electrocatalytic detection of herbicide, amitrole at $WO_3.0.33H_2O$ modified carbon paste electrode for environmental applications. Science of the Total Environment, 743 (2020) 140691.

[34] M. Pavamana, N. P. Shetti, S. J. Malode, S. D. Bukkitgar, Nano level detection and analysis of an antiviral drug at ZnO nanoparticles modified sensor, Materials Today: Proceedings, 18 (2019) 1568–1573.

[35] N. P. Shetti, D. S. Nayak, S. J. Malode, R. R. Kakarla, S. S. Shukla, T. M. Aminabhavi, Sensors based on ruthenium-doped TiO_2 nanoparticles loaded into multi-walled carbon nanotubes for the detection of flufenamic acid and mefenamic acid, Analytica Chimica Acta 1051 (2019) 58e72.

[36] N. P. Shetti, D. S. Nayak, S. J. Malode, R. M. Kulkarni, Nano molar detection of acyclovir, an antiviral drug at nanoclay modified carbon paste electrode, Sensing and Bio-Sensing Research, 14 (2017) 39–46.

[37] N. Elgrishi, K. J. Rountree, B. D. McCarthy, E. S. Rountree, T. T. Eisenhart, J. L. Dempsey, A practical beginner's guide to cyclic voltammetry, J. Chem. Educ. 95 (2018) 197−206.

[38] D. Skoog, F. Holler, S. Crouch, Principles of instrumental analysis, 6th. ed., 2007.

[39] N. P. Shetti, D. Ilager, S. J. Malode, D. Monga, S. Basu, K. R. Reddy, Poly (eriochrome black T) modified electrode for electrosensing of methdilazine, Materials Science in Semiconductor Processing, 120 (2020) 105261.

[40] J. Wang, Electroanalytical techniques in clinical chemistry and laboratory medicine, Wiley-VCH, 1988.

[41] S. D. Bukkitgar, N. P. Shetti, Electrochemical Sensor for the Determination of Anticancer Drug 5-Fluorouracil at Glucose Modified Electrode, ChemistrySelect 1 (4), (2016) 771-777.

[42] T. M. Aminabhavi, P. Munk, Preferential adsorption onto polystyrene in mixed solvent systems, Macromolecules, 12 (1979) 607-613.

[43] P. Munk, T. M. Aminabhavi, P. Williams, D. E. Hoffman, M. Chmelir, Some solution properties of polyacrylamide, Macromolecules, 13 (1980) 871-876.

[44] E. Laviron, General expression of the linear potential sweep voltammogram in the case of diffusionless electrochemical systems, J. Electroanal. Chem. 101 (1979) 19–28.

[45] A. J. Bard, L. R. Faulkner, Electrochemical Methods: Fundamentals and applications, 2nd ed., John Wiley and Sons, New York, 2004.

[46] N. P. Shetti, S. J. Malode, S. T. Nandibewoor, Electrochemical behavior of an antiviral drug acyclovir at fullerene-C_{60}-modified glassy carbon electrode, Bioelectrochemistry, 88 (2012) 76–83.

[47] R. Joseph, K.G. Kumar, Electrochemical sensing of acyclovir at a gold electrode modified with 2-mercaptobenzothiazole-[5,10,15,20-tetrakis-(3-methoxy-4-hydroxyphenyl) porphyrina to] copper(II), Anal. Sci., 27 (2011) 67–72.

[48] H. Heli, M. Yarghan, A. Jabbari, A. Parsaei, A.A. Moosavi-Movahedi, Electrocatalytic oxidation of the antiviral drug acyclovir on a copper nanoparticles-modified carbon paste electrode, J. Solid State Electrochem. 14 (2010) 787–795.

[49] M. Belter, A. Sajnog, D. Baralkiewicz, Over a century of detection and quantification capabilities in analytical chemistry – Historical overview and trends, Talanta, 129 (2014) 606-616.

[50] J. Carlson, A. Wysoczanski, E. Voigtman, Limits of quantitation–Yet another suggestion, Spectrochimica Acta Part B, 96 (2014) 69-73.

[51] D. B. Shikandar, N. P. Shetti, R. M. Kulkarni, S. D. Kulkarni, Silver-doped titania modified carbon electrode for electrochemical studies of furantril, ECS Journal of Solid State Science and Technology, 7 (2018) Q3215-Q3220.

[52] K. J. Swart, H.K.L. Hundt, A. M. Groenewald, Automated high-performance liquid chromatographic method for the determination of acyclovir in plasma, J. Chromatogr. A 663 (1994) 65–69.

[53] S. Shahrokhian, M. Azimzadeh, M. K. Amini, Modification of glassy carbon electrode with a bilayer of multiwalled carbon nanotube/iron-doped polypyrrole: Application to sensitive voltammetric determination of acyclovir, Mater. Sci. Eng. C, 53 (2015) 134–141.

[54] K. K. Peh, K. H. Yuen, Simple high-performance liquid chromatographic method for the determination of acyclovir in human plasma using fluorescence detection. J. Chromatogr. B 693 (1997) 241–244.

[55] F. Wang, L. Chen, X. X. Chen, S. H. Hu, Studies on electrochemical behaviors of acyclovir and its voltammetric determination with nano-structured film electrode, Anal. Chim. Acta, 576 (2006) 17–22.

[56] M. Sadikoglu, G. Saglikoglu, S. Yagmur, E. Orta, S. Yilmaz, Voltammetric determination of acyclovir in human urine using ultra trace graphite and glassy carbon electrodes, Curr. Anal. Chem. 7 (2011) 130–135.

[57] P. S. Dorraji, F. Jalali, Differential pulse voltammetric determination of nanomolar concentrations of antiviral drug acyclovir at polymer film modified glassy carbon electrode, Mater. Sci. Eng. C, 61 (2016) 858–864.

[58] S. Can, S. Yilmaz, G. Saglikoglu, M. Sadikoglu, N. Menek, Electrocatalytic oxidation of acyclovir on poly(p-aminobenzene sulfonic acid) film modified glassy carbon electrode, Electroanalysis, 27 (10) (2015) 2431–2438.

[59] B. Lokesh, S. Stefan, C. Sheehan, R. William, "Excipients: Background/Introduction". CRC Press, (2006).

[60] O. J. D'Souza, R. J. Mascarenhas, A. K. Satpati, B. M. Basavaraja, A novel ZnO/reduced graphene oxide and Prussian blue modified carbon paste electrode for the sensitive determination of Rutin, Science China Chemistry, 62 (2019) 262-270.

[61] G. Manasa, R. J. Mascarenhas, A. K. Satpati, B. M. Basavaraja, S. Kumar, An electrochemical Bisphenol F sensor based on ZnO/G nano composite and CTAB surface modified carbon paste electrode architecture, Colloids and Surfaces B: Biointerfaces, 170 (2018) 144-151.

Figure captions

Figure 1. Cyclic voltammograms of $K_3Fe(CN)_6$ (1.0 x 10^{-3} M)/ KCl (0.1 M) at bare GCE, ZnO/GCE, and Ca-ZnO/ GCE.

Figure 2. A) Voltammetric behaviour of ACV in pH 5.0 PBS at 0.05 Vs^{-1}; by CV technique. B) plot of pre-concentration time (0 to 60 s) Vs peak current for ACV at Ca-ZnO/GCE. C) Plot of modified amount of Ca-ZnO (0.05 µL to 0.2 µL) Vs peak current of the ACV at Ca-ZnO/GCE.

Figure 3. A) Effect of pH in the range (3.0 to 6.2) for the oxidation of ACV; accumulation time = 15 s; at Ca-ZnO/GCE. B) Plot of peak current versus pH, and C) Plot of peak potential versus pH.

Figure 4. A) Effect of sweep rate (0.01 V to 0.2 V) on voltammetric behaviour of ACV in cyclic voltammetric technique at Ca-ZnO/GCE; B) Plot of I_p/µA Vs ν/ Vs^{-1}; C) Plot of log I_p/ µA Vs log ν/ Vs^{-1}; and D) plot of E_p/ V Vs log ν/ Vs^{-1}.

Figure 5. Effect of concentration of ACV in the range (1-10: blank, 0.01 µM to 24 µM) by SWV technique in pH 5.0 PBS at scan rate 0.05 Vs^{-1}.

Figure 6. Effect of excipients on the ACV, plot of % signals versus excipients.

Scheme 1. Probable electro-oxidation mechanism of ACV.

Table 1. Comparison of LOD values for ACV at different reported methods

Table 2. Determination of ACV in pharmaceuticals and spiked human urine samples.

Figure 1

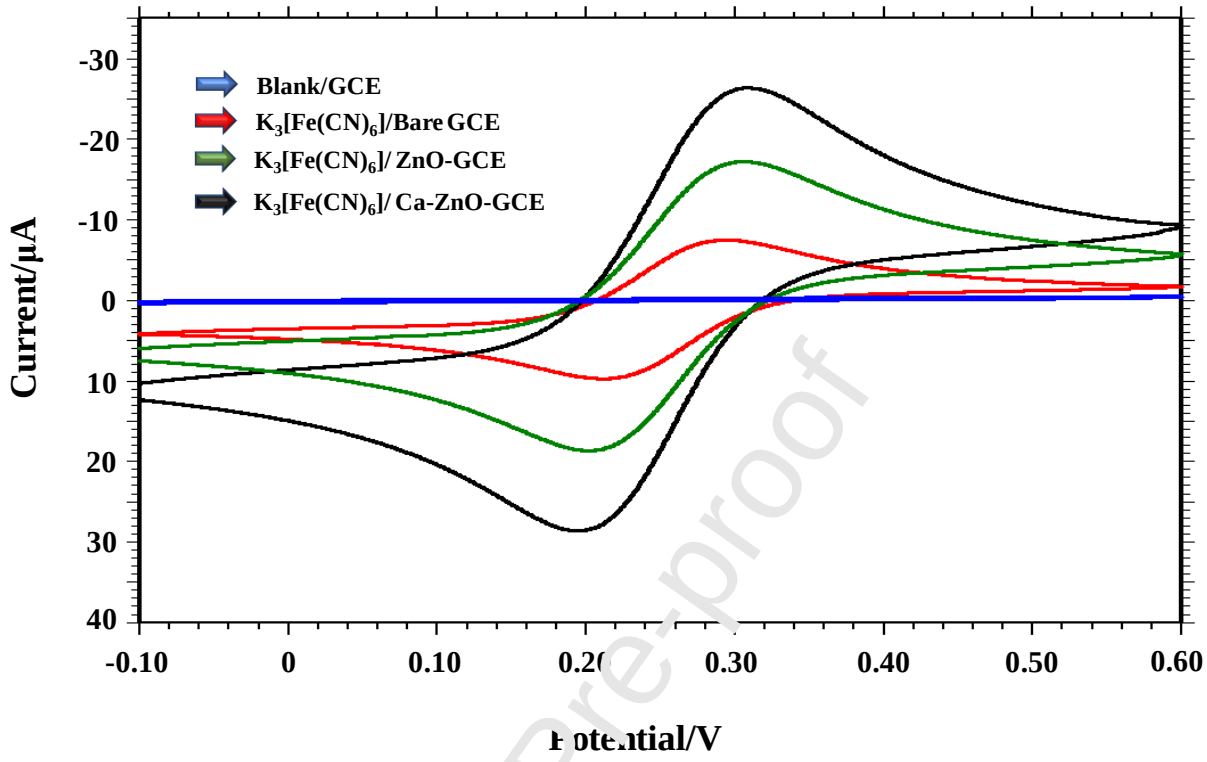

Figure 2

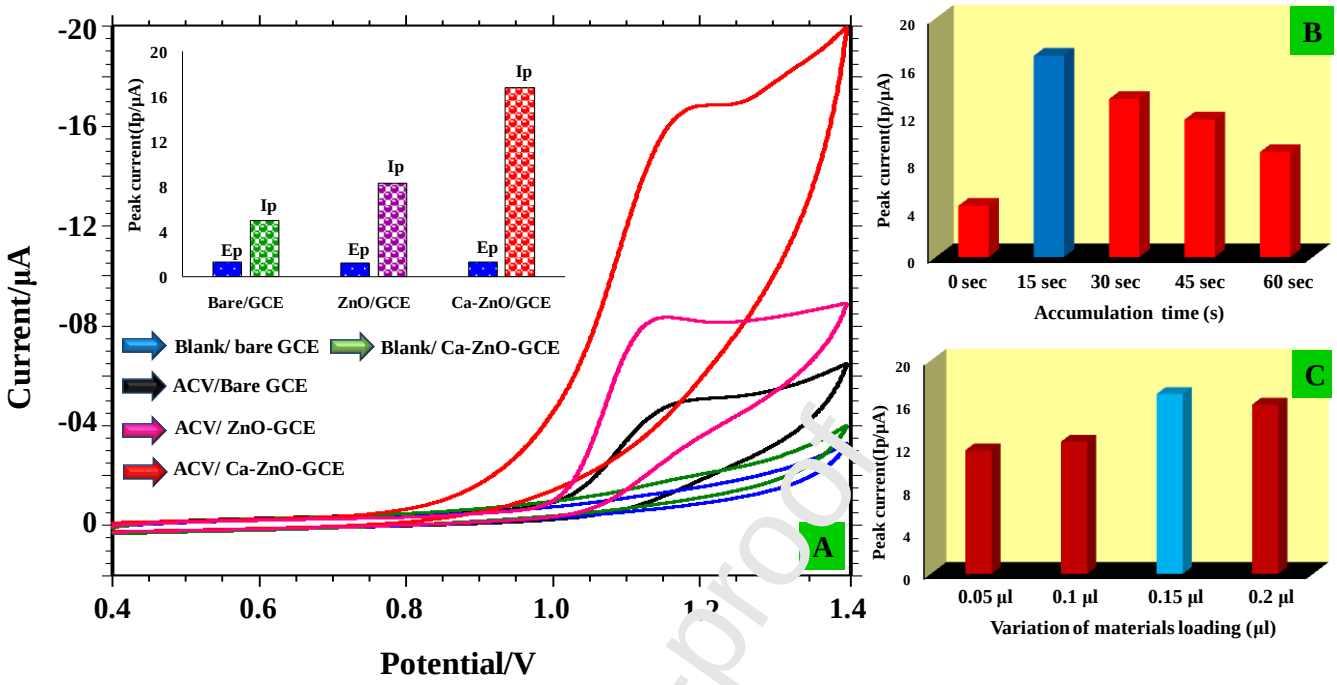

Figure 3

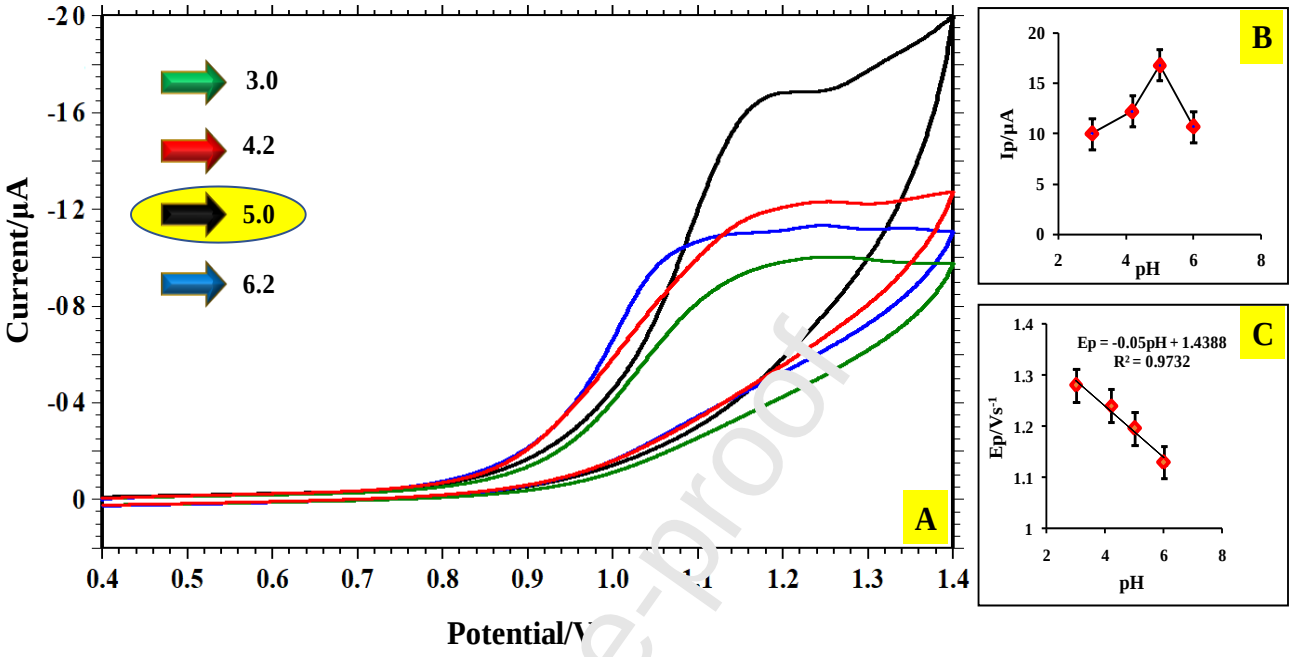

Figure 4

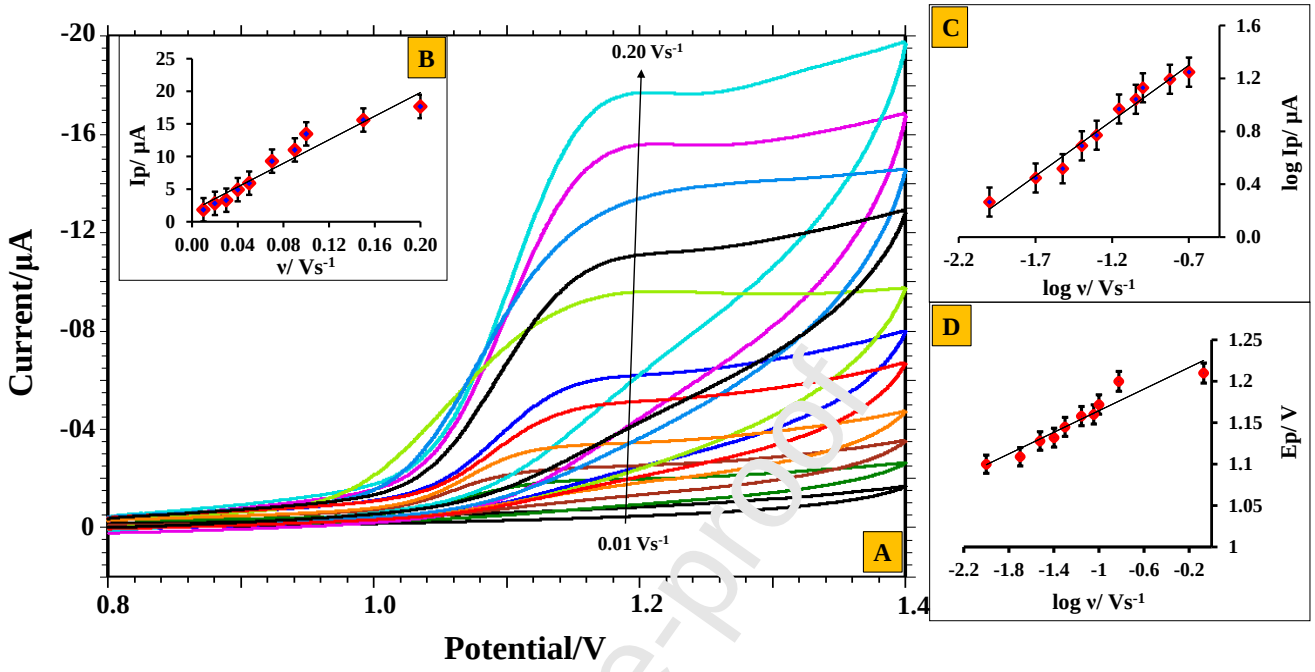

Figure 5

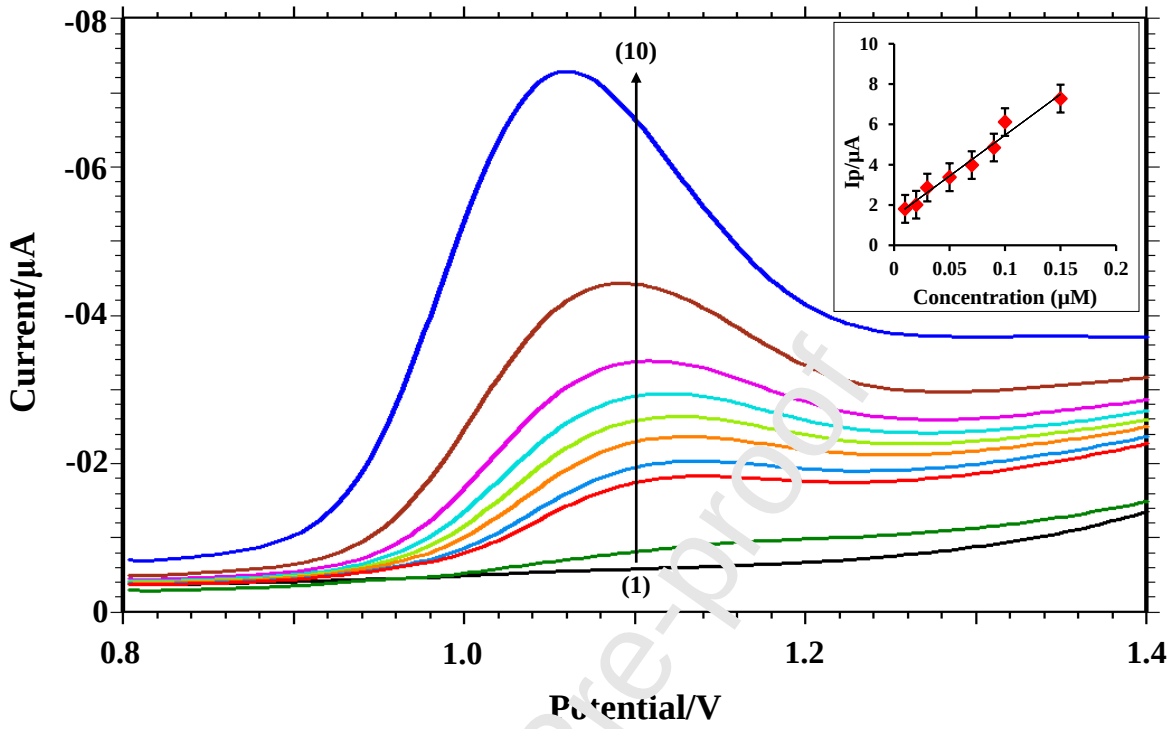

Figure 6

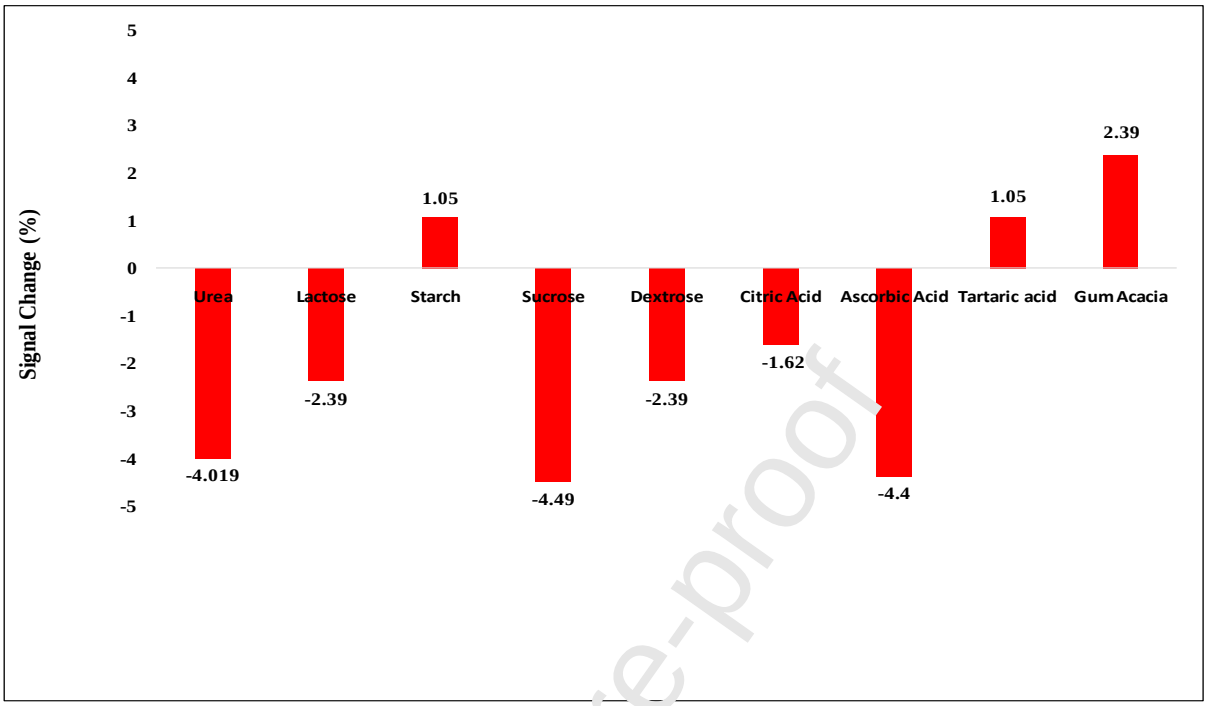

Scheme 1

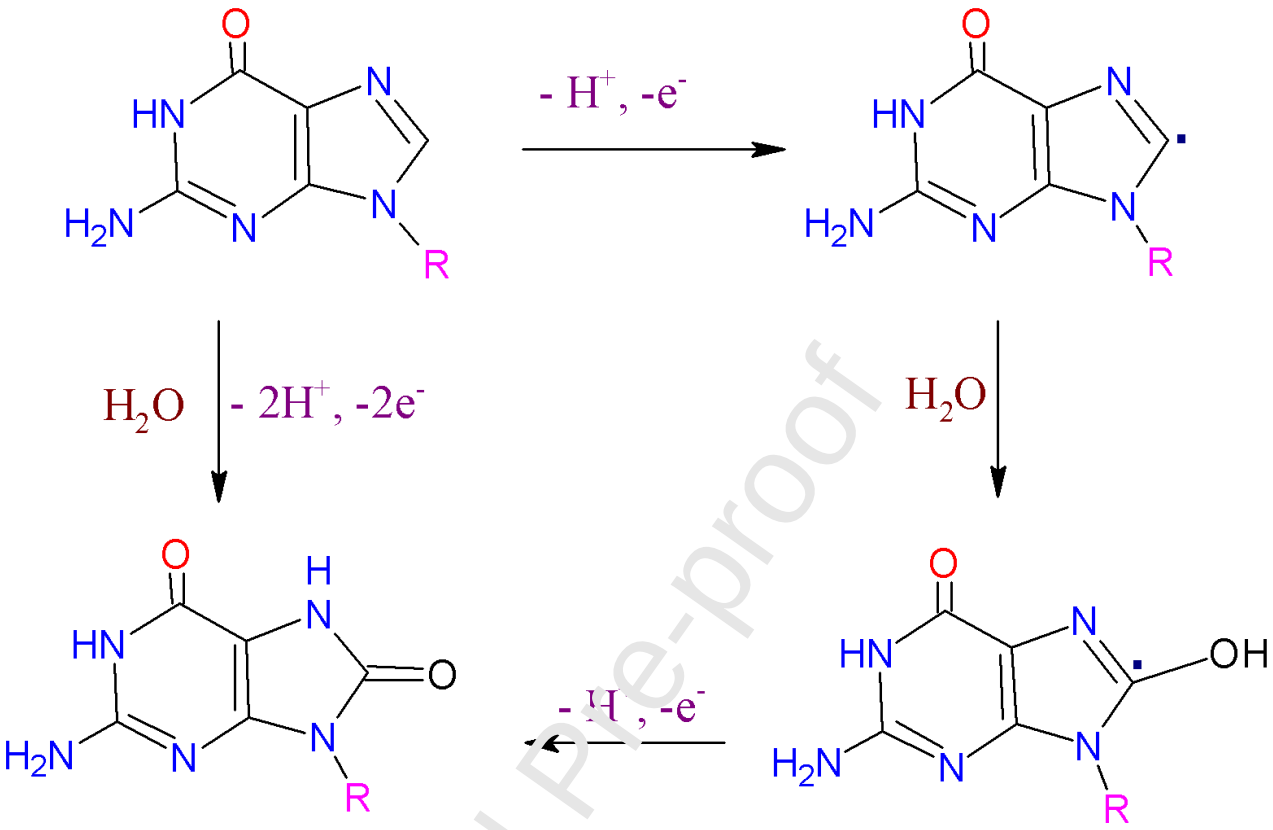

Where R = $CH_2OCH_2CH_2OH$

Table 1. Comparison of LOD values for ACV with different reported methods.

Sl. No.	Method/Electrode	LOD values	Ref
1	High Performance Liquid Chromatography	5.30×10^{-6} M	[52]
2	Linear sweep voltammetry (Multiwalled carbon nano tube/GCE[a])	1.00×10^{-8} M	[53]
3	High Performance Liquid Chromatography using florescence detector	1.30×10^{-7} M	[54]
4	Square Wave Voltammetry (ZnO[b]/GCE[a])	4.23×10^{-8} M	[35]
5	Linear Sweep Voltammetry (Multiwalled carbon nano tube -DHP[c]/GCE[a])	3.00×10^{-8} M	[55]
6	Difference Pulse Voltammetry (GCE[a])	3.50×10^{-7} M	[56]
7	Difference Pulse Voltammetry (PEBT[d]/GCE[a])	1.20×10^{-8} M	[57]
8	Difference Pulse Voltammetry (Poly(p-aminobenzen sulfonic acid)/GCE[a])	5.57×10^{-8} M	[58]
9	Square Wave Voltammetry (Ca-ZnO[e]/GCE[a])	6.18×10^{-9} M	Present work

[a]Glassy Carbon Electrode
[b]Zinc oxide Nanoparticles
[c]Dihexadecyl hydrogen phosphate.
[d]Poly Erichrome Black-T
[e]Calcium doped zinc oxide Nanoparticles

Table 2. Determination of ACV in pharmaceuticals and spiked human urine samples.

A. Determination of ACV in tablet samples by the SWV technique.				
Tablet samples	Spiked (10^{-6}M)	Detected[a] (10^{-6} M)	Recovery (%)	RSD %
1	2.0	1.98	99.00	0.5227
2	4.0	3.92	98.00	0.5280
3	6.0	5.95	99.16	0.5218
4	8.0	7.89	98.62	0.5247
Standard Deviation = 0.517, Relative Standard Deviation = 0.0528, RSD % = 0.5243				
[a] Average of five determinations				
B. Determination of ACV in spiked human urine samples by the SWV technique.				
Urine samples	Spiked (10^{-5} M)	Detected[a] (10^{-5} M)	Recovery (%)	RSD %
1	0.1	0.098	98	1.767
2	0.2	0.190	95	1.823
3	0.5	0.491	98	1.767
4	1	0.990	97	1.749
Standard Deviation = 1.730, Relative Standard Deviation = 0.0177, RSD % = 1.776				
[a] Average of five determinations				

Author Statement

The authors listed in the manuscript have contributed in this research work, and agreed to submit the manuscript to this journal.

Declaration of Interest

The authors report no conflict of interest.

Highlights

- Developed of novel Ca-doped ZnO nanoparticles for the investigation of acyclovir
- Electrode reaction mechanism followed diffusion-controlled process
- Electrocatalytic activity shows superior stability and sensitivity to electrode
- Ca-ZnO modified sensor exhibited remarkable detection limit
- Modified nanosensor is useful in pharmaceutical applications